requires fewer latches in the array (and possibly fewer latches for the skewing of coefficients if adaptive filtering is required), resulting in smaller area and power requirement. Offsetting these advantages is the decrease in throughput, because the clock speed depends on the propagation delay through a group of subcells. A simple analysis of the two classes of arrays is as follows.

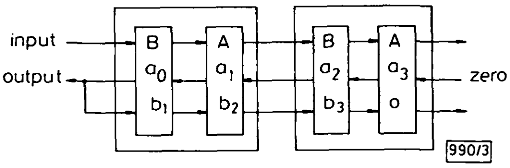

Fig. 3 *Example of a class 2 array for implementing a third-order recursive filter*

Each cell of a class 1 array has $2K + 1$ latches, so the total number of latches in the array is $(N + 1)(2K + 1)/(K + 1)$. The minimum cycle time is limited by $2(K + 1)T_a + T_m$, where T_a and T_m are the times required by a real addition and a real multiplication, respectively. Note that the multiplications can be performed in parallel. Likewise, each cell of a class 2 array has $K + 2$ latches, so that the total number of latches in the array is $(N + 1)(K + 2)/(K + 1)$. The minimum cycle time is limited by the longer of $4T_a + T_m$ and $2T_a + T_m + KT_p$, where T_p is the propagation delay from one subcell to its neighbour and should be small compared with T_a and T_m.

In general for a given K a class 2 array is preferable to the corresponding class 1 array, as a higher throughput can be attained (assuming T_a, $T_m \gg T_p$) using half the number of latches. On the other hand, one may still consider using a class 1 array if constrained by the cell library or if suitable components are available cheaply.

The critical path delay for a class 2 filter consisting of only a single cell with $K = N$ is $2T_a + T_m + KT_p$. A second-order filter implemented this way (with $K = 2$) requires six adders, six multipliers and four latches. The design in Reference 4 has a minimum cycle time of $2T_a + T_m$, but requires eight adders, eight multipliers and 16 latches, and also requires $b_1 \neq 0$.

Conclusions: Two classes of systolic array for recursive digital filtering have been presented. Both have a regular structure with uniform interconnections. The trade-off resulting from varying the degree of pipelining is discussed.

Instances of both classes of array have been captured in the μFP notation[5] and have been simulated symbolically. Algebraic theorems can be devised to derive the implementations formally. Other tools are being developed to facilitate the rapid generation of systolic structures, allowing the exploration of many design options so that the most appropriate architecture can be selected for a particular application.

Acknowledgment: This work has been undertaken as part of the UK Alvey programme (project ARCH 013), whose support is gratefully acknowledged.

W. LUK
G. JONES

28th August 1987

Programming Research Group
Oxford University Computing Laboratory
11 Keble Road, Oxford OX1 3QD, United Kingdom

References

1 KUNG, H. T.: 'Special-purpose devices for signal and image processing: an opportunity in very large scale integration (VLSI)', *Proc. SPIE*, 1980, **241**, pp. 76–84
2 LIN, H.: 'New VLSI systolic array design for real-time digital signal processing', *IEEE Trans.*, 1986, **CAS-33**, pp. 673–676
3 ROBERT, Y., and TCHUENTE, M.: 'An efficient systolic array for the 1D recursive convolution problem', *J. VLSI & Comput. Syst.*, 1986, **1**, pp. 398–407
4 KWAN, H. K.: 'New systolic array for realising second-order recursive digital filters', *Electron. Lett.*, 1987, **23**, pp. 442–443
5 SHEERAN, M.: 'Design and verification of regular synchronous circuits', *IEE Proc., E, Comput. & Digital Tech.*, 1986, **133**, pp. 295–304

AMPLIFIER-INDUCED CROSSTALK IN MULTICHANNEL COHERENT LIGHTWAVE SYSTEMS

Indexing terms: Optical communications, Crosstalk, Semiconductor lasers

When an in-line semiconductor laser amplifier is used to amplify several channels simultaneously, it can induce interchannel crosstalk if the amplifier gain is channel-dependent. It is shown that modulation of the carrier density at the beat frequency of two neighbouring channels can lead to considerable crosstalk even when the amplifier is operated well below the saturation level. An analytic expression for the channel gains of a travelling-wave amplifier is used to discuss and compare the crosstalk for ASK and FSK systems. The relatively short carrier lifetime in high-gain amplifiers may ultimately limit the channel spacing of such multichannel systems.

One of the major motivations behind the development of coherent lightwave systems is the possibility of simultaneous transmission of a large number densely packed communication channels over a single fibre.[1] The use of in-line optical amplifiers in place of regenerators is thought to be a necessity, since it provides an economical way of simultaneously amplifying all channels without the need for multiplexers.[2,3] However, the gain of an optical amplifier depends to some extent on whether a single or multiple channels are being amplified, and this leads to an interchannel crosstalk. Gain saturation is one such crosstalk mechanism, and has been extensively studied.[4–7] In this letter we discuss the implications of a fundamental mechanism that is responsible for crosstalk even when the amplifier is operated well below the saturation level. The physical mechanism behind crosstalk is modulation of the carrier density at the beat frequency of two neighbouring channels.[8] We obtain an analytic expression for the channel gain when a travelling-wave amplifier (TWA) amplifies two channels simultaneously, and use it to discuss the crosstalk for ASK and FSK formats. The crosstalk depends on the linewidth broadening factor, carrier lifetime and channel spacing. It is shown that the relatively short carrier lifetime in GaInAsP TWAs may ultimately limit the channel spacing of multichannel systems employing in-line amplifiers.

To present the results as simply as possible, we consider the case of two-channel amplification. The extension to the multichannel case is straightforward and does not change the conclusions reached here. The carrier density n inside the amplifier is obtained by solving

$$\frac{dn}{dt} = \frac{I}{qV} - \frac{n}{\tau_s} - \frac{g(n)}{\hbar\omega}\langle |E|^2 \rangle \tag{1}$$

where I is the current, V is the active volume, τ_s is the carrier lifetime and

$$E = U[E_1 \exp(-i\omega_1 t) + E_2 \exp(-i\omega_2 t)] \tag{2}$$

The angle brackets in eqn. 1 denote average over the active area, $U(x, y)$ governs the spatial distribution of the fundamental waveguide mode, and ω_1 and ω_2 are the optical frequencies of the two channels. An approximate solution of eqn. 1 is given by[8]

$$n = \bar{n} + [\Delta n \exp(i\Omega t) + \text{c.c.}] \tag{3}$$

where

$$\Omega = \omega_1 - \omega_2 \tag{4}$$

is the beat frequency. Using eqn. 3 in eqn. 1 and assuming that $g(n) = a(n - n_0)$, the DC and AC parts of n are given by

$$\bar{n} = \frac{I/I_0 + P_1 + P_2}{1 + P_1 + P_2} n_0 \tag{5}$$

$$\Delta n = -\frac{(\bar{n} - n_0)E_1^* E_2/P_s}{1 + P_1 + P_2 + i\Omega\tau_s} \tag{6}$$

where $I_0 = qVn_0/\tau_s$ is the current needed for transparency, $P_j = |E_j|^2 P_s$ is the normalised power in the jth channel, and the saturated power ($P_s \sim 1$ mW) is given by

$$P_s = \hbar\omega\sigma/(a\tau_s\langle |U^2\rangle) \tag{7}$$

where σ is the mode area.

The induced polarisation is calculated following the method of Reference 8. The carrier-density modulation affects both the gain and the index for each channel. These are given by

$$g_j = \frac{g_0}{1 + P_1 + P_2}\left[1 - \frac{(1 + P_1 + P_2 \pm \beta\delta)P_{3-j}}{(1 + P_1 + P_2)^2 + \delta^2}\right] \tag{8}$$

$$\Delta\mu_j = \frac{\Delta\mu_0}{1 + P_1 + P_2}\left[1 - \frac{(1 + P_1 + P_2 \mp \delta/\beta)P_{3-j}}{(1 + P_1 + P_2)^2 + \delta^2}\right] \tag{9}$$

where $j = 1$ or 2, $g_0 = \Gamma a n_0(I/I_0 - 1)$ is the small-signal gain, β is the linewidth broadening parameter, $\Delta\mu_0 - (\beta c/2\omega)g_0$ is the carrier-induced index change, and the parameter δ is related to the channel separation D by

$$\delta = \Omega\tau_s = 2\pi\tau_s D \tag{10}$$

In eqns. 8 and 9 the upper and lower signs are chosen for $j = 1$ and 2, respectively. Eqns. 8 and 9 include the effect of both gain saturation and carrier-density modulation.

To obtain the amplifier gain, one must in general solve the coupled wave equations for the complex fields E_1 and E_2 along the amplifier length by considering the forward and backward waves for each channel and the boundary conditions at the facets. Although this procedure is necessary for Fabry–Perot amplifiers, an approximate solution can be obtained for TWAs by neglecting the effect of facet reflections. This amounts to assuming an ideal TWA with no ripples in the gain spectrum. For this purpose, we need to solve

$$dP_j/dz = g_j P_j \qquad j = 1, 2 \tag{11}$$

where g_j is given by eqn. 8. The solution of eqn. 11 is considerably simplified if we further assume that the TWA is operated well below the saturation level, so that $P_j(L) \ll 1$, where L is the amplifier length. Assuming that the channel separation is such that $\beta\delta \gg 1$, a condition expected to be satisfied in practice, the coupled equations become

$$dP_1/dz = g_0 P_1(1 - \varepsilon P_2) \tag{12}$$

$$dP_2/dz = g_0 P_2(1 + \varepsilon P_1) \tag{13}$$

where the crosstalk parameter

$$\varepsilon = \beta\delta/(1 + \delta^2) \tag{14}$$

Eqns. 12 and 13 are readily solved to obtain the channel gains given by

$$G_1 = \frac{P_1^{in} + P_2^{in}}{P_1^{in} + \kappa P_2^{in}} G_0 \qquad G_2 = \kappa G_1 \tag{15}$$

where

$$\kappa = \exp[\varepsilon(G_0 - 1)(P_1^{in} + P_2^{in})] \tag{16}$$

and

$$G_0 = \exp(g_0 L) \tag{17}$$

is the amplifier gain in the absence of crosstalk. P_1^{in} and P_2^{in} are the channel powers at the input amplifier port. Eqns. 15 show that the channel gains are different when both channels are amplified simultaneously. In general, the longer-wavelength channel has higher gain. This feature has its origin in the four-wave mixing process.[8] More specifically, carrier-density modulation given by eqn. 3 creates gain and index gratings. The contribution on index grating, governed by the linewidth broadening factor β, is responsible for the asymmetric nature of the amplifier gain.[8]

Exprs. 15 for the channel gains can be used to discuss the dependence of the amplifier-induced crosstalk on the modulation format. A measure of crosstalk is the relative change in the amplifier gain of one channel when '1' is transmitted in place of '0' in the interfering channel, i.e.

$$C = \frac{|G_1(1) - G_1(0)|}{G_1(0)} \tag{18}$$

For the ASK format, $G_1(1)$ is given by eqns. 15 while $G_1(0) = G_0$. Using eqns. 15 and 18, the crosstalk is given by

$$C_{ASK} = \frac{(\kappa - 1)P_2^{in}}{P_1^{in} + \kappa P_2^{in}} = \frac{\kappa - 1}{\kappa + 1} \tag{19}$$

where the last expression holds for $P_1^{in} = P_2^{in}$. Using eqns. 14 and 16 and assuming that $\varepsilon G_0 P_2^{in} \ll 1$, we obtain

$$C_{ASK} \simeq \varepsilon(G_0 - 1)P_2^{in} \simeq \frac{\beta G_0 P_2^{in}}{2\pi\tau_s D} \tag{20}$$

where eqn. 10 was used together with the assumption that $G_0 \gg 1$ and $\delta \gg 1$. Clearly, crosstalk can be reduced by increasing the channel spacing D or by decreasing the interfering-channel output power $G_0 P_2^{in}$.

For the FSK format, the channel power remains the same whereas the channel spacing changes from D to $D + \Delta$ depending on the bit pattern, where Δ is the tone spacing. Using eqns. 15 and 18, the crosstalk is given by

$$C_{FSK} \simeq \frac{\beta G_0 P_2^{in} \Delta}{2\pi\tau_s D^2} \tag{21}$$

where we made the same approximations as those made in the derivation of eqn. 20. A comparison of eqns. 20 and 21 shows that $C_{FSK} = (\Delta/D)C_{ASK}$. Since generally $\Delta < D$, the crosstalk is smaller for the FSK format by a factor Δ/D.

To estimate the crosstalk level in multichannel coherent systems, consider a 1·55 μm GaInAsP amplifier with $G_0 P_2^{in} = 0{\cdot}1$ (operated 10 dB below the saturation level) and a channel spacing $D = 1$ GHz; the parameter $\beta = 6$. The carrier lifetime τ_s depends on the amplifier gain G_0. Although $\tau_s = 2$–3 ns for a GaInAsP laser, it can decrease by as much as an order of magnitude,[5] depending on the increase in carrier density which increases the Auger recombination rate considerably. Thus $C_{ASK} = 0{\cdot}05$–$0{\cdot}5$ depending on the drive current, i.e. the amplifier gain can vary by as much as 3 dB depending on the bit pattern of the interfering channel. This is indeed a large effect, and occurs even when the TWA is operated 10 dB below saturation. When the TWA operates in the saturation regime, eqns. 20 and 21 are not applicable, and eqns. 8 and 11 should be integrated numerically to obtain the channel gains. Our numerical results show that the crosstalk increases considerably in the saturation regime. In particular, the gain of the high-frequency channel can decrease by as much as 10 dB compared to the value expected in the absence of the interfering channel. This is because the four-wave mixing process initiated by the carrier-density modulation transfers significant energy from the channels to generate sidebands at frequencies $2\omega_1 - \omega_2$ and $2\omega_2 - \omega_1$.

In the analysis presented here the index change (eqn. 9) has been ignored after assuming a perfect TWA. In practice, the index changes would also induce crosstalk by coupling the channel phases. However, for closely spaced channels ($D < 10$ GHz) this crosstalk is expected to be negligible as the Fabry–Perot resonance peaks are typically separated by 100 GHz or more.

How can one reduce the amplifier-induced crosstalk in multichannel coherent systems? The only material parameters appearing in eqns. 20 and 21 are β and τ_s. However, the dependence of the crosstalk on τ_s is not fundamental. This can be seen by noting that $P_2^{in} = |E_2|^2 P_s \propto \tau_s$ from the definition of P_s in eqn. 7. Thus, for a fixed input channel power, C_{ASK} depends only on β, G_0 and D. Since β is constant for a given amplifier, the crosstalk can be reduced by operating the amplifier at a lower gain or by increasing the channel separation. The crosstalk mechanism discussed here may turn out to be the ultimate limiting factor in determining how closely two channels can be operated when in-line amplifiers are used in multichannel coherent lightwave systems.

The author is grateful to N. A. Olsson and Y. K. Park for stimulating discussions.

G. P. AGRAWAL *24th August 1987*

AT&T Bell Laboratories
Murray Hill, NJ 07974, USA

References

1 STANLEY, I. W., HILL, G. R., and SMITH, D. W.: 'The application of coherent optical techniques to wide-band networks', *J. Lightwave Technol.*, 1987, **LT-5**, pp. 439–451
2 OLSSON, N. A.: 'ASK heterodyne receiver sensitivity measurements with two in-line 1·5 μm optical amplifiers', *Electron. Lett.*, 1985, **21**, pp. 1085–1087
3 MARSHALL, I. W., O'MAHONY, M. J., and CONSTANTINE, P.D.: 'Optical system with two packaged 1·5 μm semiconductor laser amplifier repeaters', *ibid.*, 1986, **22**, pp. 253–255
4 GROSSKOPF, G., LUDWIG, R., and WEBER, H. G.: 'Crosstalk in optical amplifiers for two-channel transmission', *ibid.*, 1986, **22**, pp. 900–902
5 SAITOH, T., and MUKAI, T.: '1·5 μm GaInAsP traveling-wave semiconductor laser amplifier', *IEEE J. Quantum Electron.*, 1987, **QE-23**, pp. 1010–1020
6 EISENSTEIN, G., HALL, K. L., JOPSON, R. M., RAYBON, G., and WHALEN, M. S.: 'Two-color gain saturation in an InGaAsP near-traveling-wave optical amplifier'. OFC/IOOC '87, 1987, Paper ThC4
7 WESTLAKE, H. J., and O'MAHONY, M. J.: 'Bidirectional and two-channel transmission system measurements using a semiconductor-laser amplifier repeater', *Electron. Lett.*, 1987, **23**, pp. 649–651
8 AGRAWAL, G. P.: 'Four-wave mixing and phase conjugation in semiconductor laser media', *Opt. Lett.*, 1987, **12**, pp. 260–262

UNIFIED APPROACH TO DETERMINATION OF MODES IN CYLINDRICAL CAVITIES AXISYMMETRICALLY LOADED WITH DIELECTRICS

Indexing term: Dielectrics

Based on a variational expression, a unified approach for the determination of all modes in cylindrical cavities axisymmetrically loaded with dielectrics is presented. This approach employs one-dimensional finite-element basis functions along the *r*-axis, and uses a penalty term to alleviate the resulting spurious modes. Using this technique, the resonant frequencies of several cavities are calculated.

Introduction: Recent advances in the development of very low-loss dielectric materials with high dielectric constants have paved the way for the design of compact cavity filters. Applications of these filters are widespread, especially in satellite communications, where the emphasis is on high-quality, low-weight and small-size filters.

Unlike empty cavities, the determination of modes in dielectric-loaded resonators is not straightforward, and usually requires some computational effort. Several techniques, including the mode matching and finite-element methods, have so far been applied to analyse modes in cyclindrical cavities axisymmetrically loaded with dielectrics.[1–4] However, some of these techniques are used to find only one category of modes in these resonators.[2,3] Those dealing with all modes (i.e. TE, TM and hybrid modes) are nevertheless found to be restricted to very simple dielectric-loaded cylindrical cavities in practice.[1,4]

The work presented in this letter is the result of a need for a flexible but powerful method for a unified treatment of all modes in cylindrical cavities loaded axisymmetrically with dielectrics. The developed technique can be easily extended to resonators loaded with many dielectrics, and is distinctly efficient for cavities in which dielectrics are fully extended along the cavity length.

Theory: Modes in a cavity resonator can be determined using the vector functional

$$\omega^2 = \frac{\iiint_V \nabla \times \boldsymbol{H}\varepsilon^{-1}\nabla \times \boldsymbol{H}^*\, dv + \alpha \iiint_V |\nabla \cdot \boldsymbol{H}|^2\, dv}{\iiint_V \boldsymbol{H}\mu \boldsymbol{H}^*\, dv}$$

where ω is the angular resonant frequency, V the volume of the cavity, $\boldsymbol{H}$ the magnetic field inside the cavity and the asterisk denotes complex conjugate.

The above expression is the result of the addition of a penalty term to the well known magnetic vector functional given by Berk.[5] Providing there is a sufficiently large penalty parameter α, the penalty term in eqn. 1 would ensure a divergence-free solution for $\boldsymbol{H}$.[6]

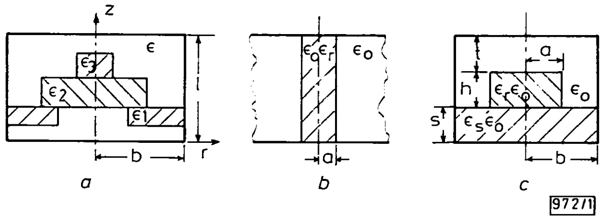

Fig. 1

a Cross-section of a cylindrical cavity resonator axisymmetrically loaded with dielectrics
b, c Cross-sections of resonators analysed in this letter

In a cylindrical cavity resonator axisymmetrically loaded with dielectrics (Fig. 1*a*), components of the magnetic field can be expanded as follows:

$$H_z = \begin{Bmatrix} \cos m\theta \\ \sin m\theta \end{Bmatrix} \sum_{p=1}^{P} \sum_{n=1}^{N} A_{pn} N_n(r) \sin (p\pi z/l) \tag{2}$$

$$H_r = \begin{Bmatrix} \cos m\theta \\ \sin m\theta \end{Bmatrix} \sum_{p=0}^{P} \sum_{n=1}^{N} B_{pn} N_n(r) \cos (p\pi z/l) \tag{3}$$

$$H_\theta = \begin{Bmatrix} \sin m\theta \\ \cos m\theta \end{Bmatrix} \sum_{p=0}^{P} \sum_{n=1}^{N} C_{pn} N_n(r) \cos (p\pi z/l) \tag{4}$$

where $N_n(r)$ is a first-order, finite-element basis function. Substituting the above expressions in eqn. 1 and applying the Rayleigh-Ritz procedure, the resonant frequencies of all modes in the cavity can be determined. The associated fields can subsequently be evaluated. Examination of eqns. 2–4 reveals that the expansion of the $\boldsymbol{H}$ field in the given form is computationally advantageous for solutions of dielectric-loaded cylindrical cavities whose dielectrics are fully extended along the cavity length. This is because for these cavities, owing to the

Table 1 RESONANT FREQUENCIES OF VARIOUS MODES CALCULATED BY DIFFERENT METHODS FOR STRUCTURE SHOWN IN FIG. 1*b*

Mode	Present tech.	Ref. 4	Ref. 8	ε_r
	GHz	GHz	GHz	
TE_{011}	4·229	4·219	4·221	35·63
TE_{021}	6·035	6·031	6·026	35·48
TE_{031}	8·265	8·245	8·241	35·39
TE_{041}	10·681	—	10·636	35·35
TM_{011}	4·488	4·377	4·478	37·31
TM_{021}	6·630	6·573	6·603	36·61
HEM_{111}	3·842	3·561	3·839	34·63
HEM_{121}	4·977	4·969	4·967	35·39
HEM_{131}	5·305	5·160	5·488	36·33
HEM_{141}	7·079	7·013	7·047	35·37
HEM_{211}	4·561	4·366	4·608	33·65
HEM_{221}	5·760	5·705	5·754	35·15

$a = 9{\cdot}525$ mm and $l = 7{\cdot}62$ mm